Digest Journal of Nanomaterials and Biostructures Vol. 10, No. 4, October - December 2015, p. 1439 - 1447

STRUCTURAL AND THE CORROSION CHARACTERISTIC STUDY OF AZ91 ALLOY WITH AND WITHOUT CuZn COATING IN %3 NaCl SOLUTION

M. Y. HACIIBRAHIMOĞLU[a], M. BEDIR[b*], M. ÖZTAŞ[c], C. CAKEZ[b]
[a]*Gaziantep University, Department of Metallurgical and Materials Science Engineering, 27310 GAZİANTEP*
[b] *Gaziantep University, Department of Engineering Physics, 27310 GAZİANTEP*
[c]*Yalova University, Department of Chemical and Process Engineering, YALOVA*

The corrosion characteristics and the structural properties of electrodeposited CuZn on AZ91 alloy were investigated. The surfacemorphology and compositions were analyzed by SEM, EDX and XRD results. The XRD pattern showed Zn and ε-phase CuZn polycrystalline hexagonal close packed phase. The corrosion potential of CuZn electrodeposited AZ91 alloy was changed with the immersion time in %3 NaCl solution. Cyclic Voltammetry results presented that the three peaks were observed in cathodic region for the reduction of Cu(II) ions to Cu(0)and the one in anodic region for electrochemical co-reduction of the Zn(II) and Cu(II) ions. The CuZn-based coating improved the corrosion resistance of AZ91 alloy.

(Received October 9, 2015; Accepted December 19, 2015)

*Keywords:*Electrodeposition**,** XRD,SEM, Corrosion

1. Introduction

AZ91 consisting mainly of %90Mg, %9Al and %1Zn[1], is a part of AZ family used in the field of transportation [aerospace, automobile etc.], agriculture, chemical, construction and energy industries owing to its impressive efficient properties such as castability, weldabilty, good machinability, rigidity, toughness, lightness. The usage requirement of on demand is clearly open for the future. One important point is the density of magnesium in comparison with that of other elements such as 35% lighter than aluminum and four times lighter than steel [2,3]. In addition, the use of magnesium is its engineering metallic characteristics related to the corrosion potential means that magnesium is more active overall than other engineering metals. Through alloying, the physical and chemical performance of pure Mg is significantly increased. Magnesium alloys are light, structural and functional engineering materials with a high strength to weight ratio. The high chemical activity of Mg corresponds to a negative standard equilibrium potential of Mg, ca. -2.4V [4-9]. This standard equilibrium potential is more negative than any other engineering metal including coatings. A stable and protective passive film forming on the surfaces of these metals significantly inhibits the anodic process and thus results in a positive corrosion potential. Unfortunately, the surface films formed on Mg and its alloys are generally unprotective and the anodic polarization resistance is low. Therefore, in a corrosive environment, the corrosion potentials of Mg and its alloys are as negative as –1.7 – –1.6 V/ NHE [9].

In this study the morphological and the corrosion behavior of AZ91 (the chemical compositions of AZ91 are given in Table 1) were examined under different immersion time in %3 NaCl solution. There are many studies on AZ91 rather than on other AZ-series such as AZ21, AZ31, AZ61, AZ63, AZ80 etc. [1,10-13]. This magnesium alloy has hexagonal-close-packed (h.c.p) crystal structure. According to its restriction of slip system there are not much deformation leading to the limitation of deformability and work strengthening [14]. During surface treatment working of AZ91 substrate CuZn alloy is used. Copper and copper base alloys (e.g.: CuZn) are

*Corresponding author: bedir@gantep.edu.tr

used in many environments and applications. They resist many saline solutions, alkaline solutions, and organic chemicals. The corrosion behavior of these alloys can be better understood by examining the potential-pH diagram for copper. Copper is a relatively noble metal compared with iron. The immune region for copper extends to cover mildly oxidizing conditions. Copper-base alloys are immune from corrosion in environments such as deteriorated HCl, but the addition of oxygen or other oxidizing species will cause corrosion. Furthermore, copper exhibits a passive range from neutral to mildly alkaline conditions, that is, conditions of pH 7 to 12. In such solutions, copper will be thermodynamically stable (immune) under reducing conditions. Copper-base alloys corrode in oxidizing acids and in strongly alkaline solutions [15]. Therefore our investigation was intensively around high pH values for coating.

Table 1. The content of AZ91

AZ 91	
Mg	89.445
Al	9.089
Zn	0.882
Mn	0.445
Si	0.11
Fe	0.018
W	0.009

Besides the analysis of composition and resistivity characteristics of AZ91 alloy with and without CuZn coating against corrosion, required experiments were carried out to get the profound information about metallurgical behavior of this alloy.

2. Experimental procedure

The disc shape of working electrode AZ91 alloy substrates having the diameter of exposed area 1cm^2 was covered with the method by which molded compressed and heated bakalite. This is a conventional way to isolate other parts of AZ91 alloy substrate from electrolyte then the surface of substrate was polished with Struers-Laboforce-3 polishing set. CuZn alloy was grown on the surface of the substrate by using traditional three electrode system. To grow of the CuZn alloy, the chemical solutions were prepared using analytical grade chemicals (Merck, Sigma Aldrich) and double distilled water. The compositional chemical salt list is given in Table 2. The pH value of the chemical solution (pH=9.2) was adjusted with a few drops of NaOH (%50wt.). The electrochemical behaviors of the electrodeposited AZ91 alloys before and after coating were analyzed in solution of 3wt% NaCl at pH 6.8 and at room temperature in the same Pyrex glass cell. In every before-after measurement steps the specimens were dried and ground with different high sensitive abrasive SiC papers and cleaned in DD-water and dried in hot air.The quantitative composition analysis of the electrodeposits was examined by Jeol JSM 6390 LV scanning electron microscope (SEM) with energy dispersive spectrometer (EDS) working at 15-30 kV. Preferential crystal orientations of the deposits on the steel surface were determined by X-ray diffraction (XRD) analysis, using a Philips PAN-alyticalX'Pert Pro X-ray diffractometer with CuK-α radiation (1.5418A). The 2θ diffraction angle range of 10^o–90^o was recorded at a rate of 0.02^o 2θ/0.5 s. The crystal phases were identified comparing the acquired 2θ values and their intensities. The potentiodynamic measurements for cyclic voltammetry and linear sweep voltammetry were examined to obtain the corrosion characteristics of both alloys.

Table 2. Content of chemical solution

Solution	Amount (in mol / lt)	Amount (in g.)
$K_4P_2O_7$	0,4	29,77
$ZnSO_4.7H_2O$	0,1	5,74
KH_2PO_4	0,5	1,95
$CuSO_4.H_2O$	0,01	0,5

3. Results and Discussion

3.1. Scanning Electron Microscope Analysis (SEM)

As shown in Fig. 1 the detailed surface characteristics of CuZn coated AZ91 alloy presents uniformly distributed spherical particles and shows the range of particle sizes about average diameter of 1 μm with the aid of SEM analysis.The intermetallic precipitates are still visible by SEM, because of the different morphology of the coating formed on the matrix and on the intermetallic group. While the coating on the precipitate looks compact and uniform, the coating on the matrix appeared uncracked and regular. The high crystallinity of the CuZn coated surface can be also seen from SEM image. This is supported by XRD analysis containing narrow-high peak intensity.

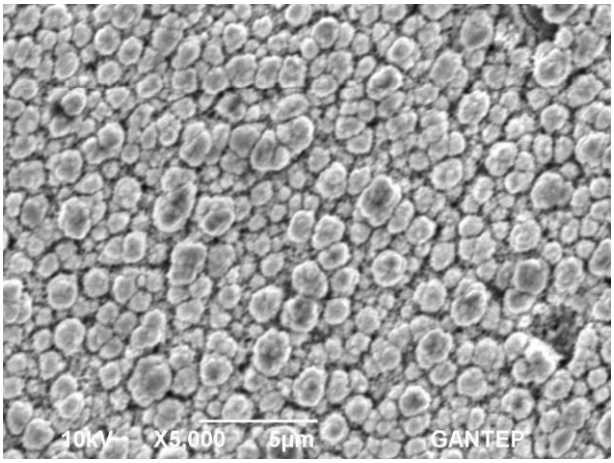

Fig. 1. The picture of the grain distribution on one CuZn coated AZ91 specimen obtained by SEM analysis

3.2. X-ray Diffraction and EDX Analyses

X-ray diffraction patterns of Cu–Zn deposits on AZ91 substrate are represented in Fig. 2. The peak intensity isobserved to be high for Zn and CuZn that indicates a better crystallinity and the formation of more crystallites with well-defined orientation (002) and (100) plane of hexagonal phase. The interplanar distances, $d_{(hkl)}$ were compared with the expected values for the phases described in JCPDS [21]. The dominant crystal orientation of the electrodeposits depends on the experimental conditions such as pH, current density and temperature. The XRD pattern also shows the formation of lines corresponding to of Zn phase and hexagonal close packed ε-phase CuZn phase with different crystallographic orientations and the films are polycrystalline structure. The surface layer is formed with one phase CuZn (ε-phase-hexagonal). The Zn concentration is more in the initial CuZn alloy solid solution and the radius of Zn atom is larger than that of Cu atom, this is a cause of the expansion of the lattice of the initial CuZn alloy along with the decrease in d-spacing and the increase in the diffraction angle, as shown in the Table 3 proving the inverse relationship between d and diffraction angle. The intensity of the diffraction peaks of CuZn phase is very low compared with those of other phases of Zn relatively. The highest intensity peaks were

observed at angles (in 2θ) of 34.74, 36.98 and 43.45. These were indexed to diffractions from the (002), (100) and (101) planes of Zn, Cu_4Zn and Cu_4Zn respectively. There are also lower intensity peaks observed at angles (in 2θ) 32.56, 48.27, 57.34, 63.65, 69.26 and 72.785. These were indexed to diffractions from the (100), (102), (102), (103), (110) and (110) planes of Zn, $Mg_{0.97}Zn_{0.03}$, Cu_4Zn, $Mg_{0.97}Zn_{0.03}$, Cu_4Zn and Zn respectively. It is also observed that each of these peaks have neighbor hills beside, because of the existing adjacent peaks. The observed phase is in accordance with what one would expect from the binary equilibrium diagram of the Cu–Zn system.One can see in the figure 2 that the observed third and fourth peaks can be indexed to diffractions from the intermetallic ε phase of CuZn which is known to have the composition $Cu_{0.8}Zn_{0.2}$. XRD peaks corresponding to the Cu-rich intermetallic ε phases were also observed. The observed phase is in accordance with what one would expect from the binary equilibrium diagram of the Cu–Zn system [15-20].The peak intensity is observed to be high for Zn and CuZn that indicates a better crystallinity and the formation of more crystallites with well-defined orientation in (002), (100), (101) and (103) planes of hexagonal phase. From the EDX spectra in fig. 3 and the EDX analysis report in table 4, it is seen that the concentration of Zn about 0.1 M and the concentration of Cu about 0.01 M in the growth solutions after the growth process on the surface of the AZ91 substrate with doping values of Zn and Cu at 83.118 (%wt) and 16.574 (%wt) in the films, respectively. The film morphology did not change and is uniform. The particle sizes of the structures are about 1 μm calculated by a pixels analysis program. On the other hand, the particles started to form aggregates on the surface and therefore the surface of the films became relatively smooth which means the porosity was decreased at higher doping Zn percentages [22- 26].

Table 3. XRD data of 3 high intensity peaks of CuZn coated AZ91 substrate

Substance	***hkl***	2θ	$d_{(hkl)}(A^o)$
Zn	(002)	34.74	2.5797
Cu_4Zn	(100)	37.12	2.4199
Cu_4Zn	(101)	43.65	2.0717
Cu_4Zn	(102)	58.10	1.5861
Cu_4Zn	(101)	43.45	2.0806

Table 4. Quantitative values of CuZn alloys after coating on AZ91 substrate

Elt.	**Line**	**Intensity (c/s)**	**Concentration (%)**	**Units**
Al	Ka	1.87	0.309	wt.%
Cu	Ka	33.27	16.574	wt.%
Zn	Ka	119.59	83.118	wt.%
			100.000	wt.%

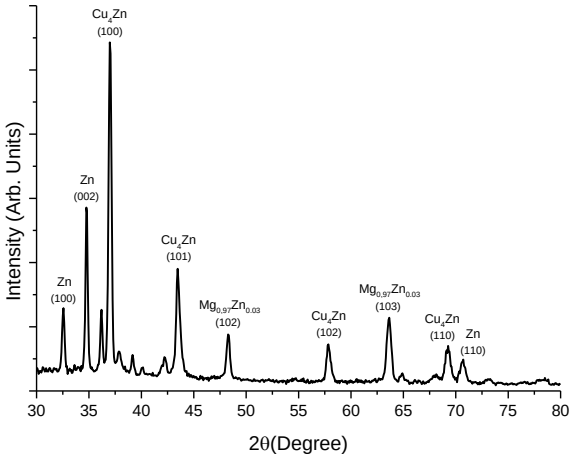

Fig. 2. XRD pattern of ZnCu alloy growth on AZ63 substrate deposited by electrodeposition technique

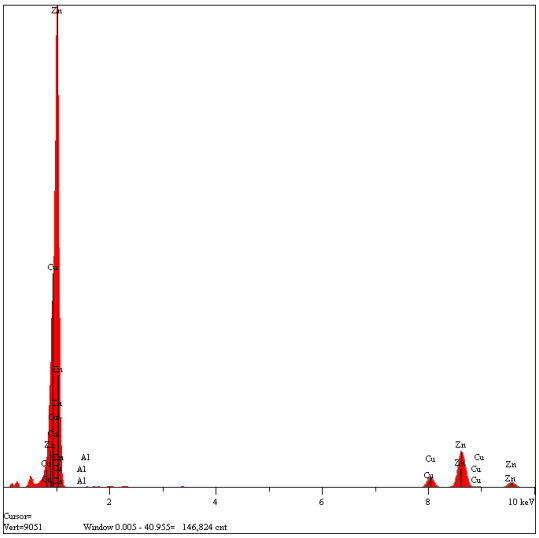

V = 15.0 kV Takeoff Angle = 35.0° Elapsed Live Time =100.0 s

Fig. 3.SEM images of the surface morphology and EDX spectra of CuZn.

3.3 Cyclic Voltammetry Analysis

The cyclic voltammetry measurement for CuZn coated on AZ91 alloy substrate was performed within the potential range of -2.5 to 0.5 V using platinum electrode. The potential scan was initiated in the negative direction from the open-circuit potential (EOCP = -0.2 V) at a scan rate (*v*) of 0.1 mV/sec. The cathodic part of the curve in Fig.4 exhibits the peak A EPA = -0.746 V, which is associated with the reduction of Cu (II) ions to Cu (0). This result is supported by previous studies [27] demonstrating that the electrodeposition process is from reduction of the Cu complex. The anodic part of CV curve shows a fast increase in the cathodic current due to the growth of the nucleation process [28] where the electrochemical co-reduction of the Zn (II) and Cu (II) ions are carried out at point B (0.193 V). It is mentioned that if during the alloy formation by via electrochemical, at least one metal is electrodeposited, this is a factor for the possible formation of intermetallic compounds. The point C is the inversion of the positive potential scan at 0.500 V. The peak D (-0.589 V) is associated with the oxidation of Cu electrodeposited during the

potential scan in negative direction. While there is a presence of three peaks A, B and C in the cathodic scan range; the anodic part of this voltammogram indicates one peak D, associated to the dissolution of phase of CuZn alloy. According to the literature, the phases formed in the CuZn by via electrochemical differ from those in metallurgical method [29, 30], and the results showed the coexistence of intermetallic compounds CuZn.

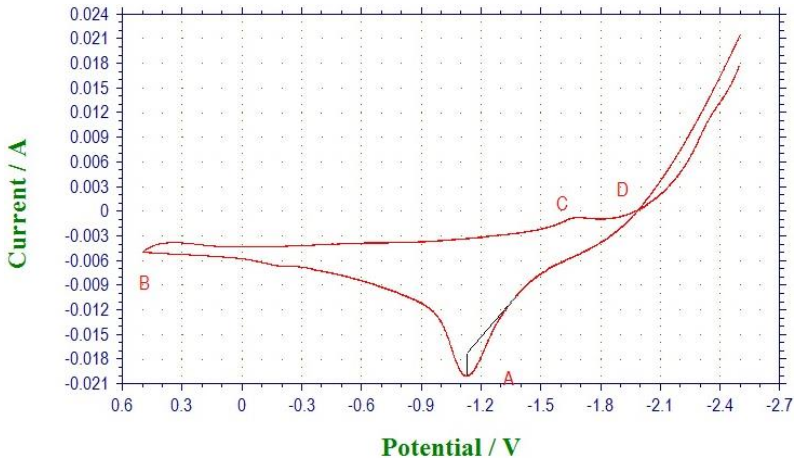

Fig. 4.Comparison of the voltammograms of uncoated AZ91 obtained from electrolytic solution at fixed potential (-2 V). Scan rate (v) of 0.1 V/Sec.

3.4 Linear Sweep Voltammetry Analysis of Uncoated and CuZn coated AZ91

The potentiodynamic polarization curves for uncoated AZ91 alloy are shown in Fig.5 with different immersion durations in solution of 3wt% NaCl at pH 6.8 and at room temperature. Most of the curves exhibit a generally expected shape with a plateau extending on the anodic potential domain. As seen from Fig.5 the cathodic polarization curves mainly represent the cathodic hydrogen evolution, the corrosion current density (I_{corr}) and potential can be readily calculated by Tafel plot. The longer immersion times shifted their curves to smaller current densities, possibly associated with the formation of a high-protective oxide layer resulting in the high potential resistance, which does not impede the corrosion attack progression. The corrosion characteristic of AZ91 alloy revealed a clearly shift of E_{corr} towards more noble values and pointed the most significant change on the E_{corr} values, possibly due to the high reactivity of this alloy which promotes formation of a gradually thick corrosion layer, limiting the attack progression. The evolution of the electrochemical behavior of uncoated AZ91 alloy with 30 min. immersion reveals E_{corr} at around -1.685 V ($I_{ox} = I_{red}$) in Figure 5. The passivity is between -1.685 and +0.500 V. The fast corrosion is started from -2.00V till -1.685V in cathodic region in which the current lies between +8.2.6mA and -1.794μA ($I_{ox}>I_{red}$). After -1.685 V to the left side, one can see the passivation region with the found current from -1.794μA to around -1.11mA ($I_{red}>I_{ox}$). From Fig.6, it can be stated that the characteristic of coated AZ91 for 30 min is definite identifiable as expected that means the corrosion potential is at around -1.730 V and at negative side with current value of -0.6901μA of the related Tafel slope. As the potential characteristic of uncoated 60 min measurement in Fig.5 is noted at -1.638V then that of the coated measurement shows low potential value in the same region (E_{corr} at around -1.620V). The corrosion is started from -1.620 V till -0.500 V in cathodic region in which the current lies between -0.0618μA and -0.6654μA ($I_{ox}>I_{red}$). After -1.620 V on the left side, one can see passivation region with the found current from -0.6654μA to around and -0.0726 μA ($I_{red}>I_{ox}$). The above differences in the corrosion potential and the corrosion current density are responsible for a weak corrosion resistance for the CuZn coated AZ91 sample in the %3 NaCl solution at 60 min. immersion time. But for the measurements of 90 min. immersion it can be seen that the corrosion characteristic between uncoated and CuZn coated AZ91 alloy has high difference. Corrosion resistance for uncoated AZ91 alloy is -1.462 V but for CuZn coated is 1.256 V in anodic region. This attributes that a high

corrective CuZn surface occurred with the thin passive oxide film on CuZn which is responsible for better corrosion resistance. The final measurements of potentiodynamic polarization for 120 min. immersion time show that the corrosion potential is at -0.053 V for uncoated and is at +0.518Vfor coated, as given in Table 5. The corrosion characteristic of CuZn coated AZ91 alloy shifts slowly to the anodic region which is attributed that this shifting is evidence in the forming of a thin high passive oxide film on the CuZn film and also on the AZ91 alloy related to the increase in the immersion time in %3 NaCl solution.

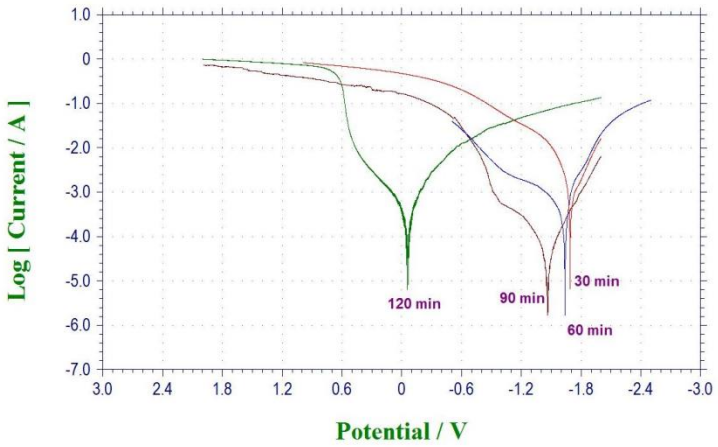

Fig. 5.all potentiodynamic polarization curves of uncoated AZ91 alloy in %3 NaCl for 30, 60, 90 and 120 minutes

Table 5. The immersion time of uncoated and coated AZ91 vs. E_{corr} for that of AZ91 Alloy

Duration in (%3)NaCl	E_{corr}(V) uncoated	E_{corr}(V) coated
30 min.	-1.685	-1.730
60 min.	-1.638	-1.620
90 min.	-1.462	+1.256
120 min	-0.053	+0.518

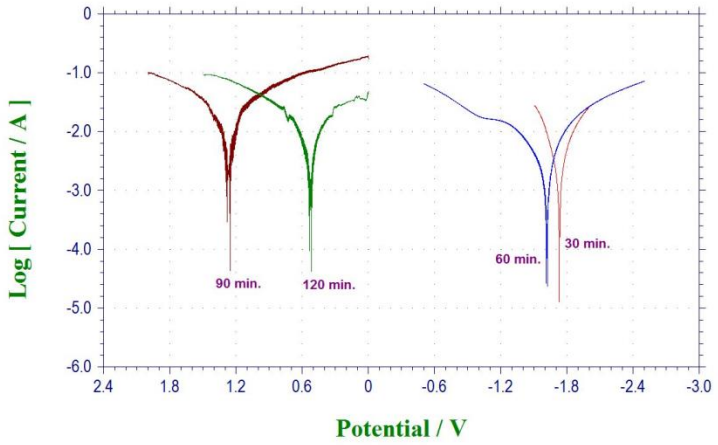

Fig. 6all potentiodynamic polarization curves of coated AZ91 alloy in %3 NaCl for 30, 60, 90 and 120 minutes.

4. Conclusion

The morphological structure and the corrosion behavior of AZ91 under different immersion time in %3 NaCl solution at pH=6.8 at room temperature were examined.

Uniformly distributed spherical particles having about average diameter size of 1 μm from the CuZn coated AZ91 surface were determined with the aid of SEM analysis.

From X-ray diffraction patterns of Cu–Zn deposit, better crystallinity and the formation of more crystallites with well-defined orientations of hexagonal phase were determined by XRD analysis.

The Zn 83.118 (%wt) and Cu 16.574 (%wt) concentrations in growth solutions after the growth process on AZ91 substrate surface were carried out with the aid of EDX method.

The cyclic voltammetry measurements gave that there was a presence of three peaks, A associated with the reduction of Cu (II) ions to Cu (0), B associated with the electrochemical co-reduction of the Zn (II) and Cu (II) ions and C which was cathodic part of the curve; the anodic part of this voltammogram indicated one peak D associated with the oxidation of Cu during electrodeposition process.

The corrosion resistivities of the samples showed tendency shifting from low potential values to the higher one, depending on relatively increasing the immersion time in %3 NaCl solution. According to those results, electrodeposited CuZn alloy film is a suitable coating substance for AZ91 alloy to increase the resistivity against the corrosion.

Acknowledgements

This study is supported by University of Gaziantep, Scientific Research Projects Unit (BAPYB) by a research project number of MF.09.07.

References

[1] G. L. Song, Atrens, A, Corrosion Mechanisms of Magnesium alloys Advanced Engineering Materials **1(**1),11(1999).
[2] G. L. Song, Atrens, Understanding Magnesium Corrosion Advanced Engineering Materials, **5** 12 (2003)
[3]M.K.Külekçi, Magnesium and its alloys applications in automotive industry, **39**(9-10)851 (2008)
[4]M.Gupta, Magnesium, Magnesium alloys, and Magnesium composites, New Jersey: Wiley,2011
[5] Perrault G.G. Magnesium, Encyclopedia of electrochemistry of the elements, Wiley, **8**, 263 (1978)
[6] G. –L.Song, D.St. John, Materials and Corrosion **56**(1)a:15 (2005).
[7] F.-H. Cao, V.-H.Len, Z. Zhang, and J.-Q. Zhang Corrosion Behavior of Magnesium and Its Alloy in NaCl Solution Russian Journal of Electrochemistry (2009)
[8]Bard A.J., Faulkner L.R., Electrochemical Methods, Fundamentals and Applications, John Wiley, 1980
[9] Song G. –L, Corrosion of Magnesium alloys, Woodhead, Cornwall, UK, 2011
[10] G.Song, Corrosion behaviour of AZ21, AZ501 and AZ91 in sodium chloride, Corrosion Science, **40(**10),1769 (1998)
[11] Pardo, M.C. Merino, A.E. Coy, R. Arrabal, F. Viejo, E. Matykina, Corrosion Science **50**, 823 (2008)
[12] C.S. Lin, H.C. Lin, K.M. Lin,W.C. Lai, Corrosion Science, **48(**1), 93(2006).
[13] Feliu,S et al., Applied Surface Science, **255(**7), 4102 (2009).
[14] Y.Z. Lü, Q.D. Wang, W.J. Ding, X.Q. Zeng, Y.P. Zhu, Materials Letter, **44**, 265(2000).
[15] J. R.Davis, Corrosion Understanding the Basics, ASM International, pp:266, Ohio, USA, 2000

[16] RasimÖzdemir, ˙Ismail HakkıKarahan, Applied Surface Science **318**,314 (2014).
[17] LayaDejam, S. Mohammad Elahi, ,Molecular Crystals and Liquid Crystals, **577**(1), 59,(2013)
[18] Marcos F. de Carvalho, Elton P. Barbano, Ivani A. Carlos, Surface & Coatings Technology **262,** 111(2015).
[19] Nasser K. Awad, E.A. Ashour, Nageh K. Allam, Applied Surface Science **346,** 158(2015).
[20] Akira Nagaoka, RyojiKatsube, Shigeru Nakatsuka, Kenji Yoshino, Tomoyasu Taniyama, Hideto Miyake, Koichi Kakimoto, Michael A.Scarpulla, Yoshitaro Nose, Journal of Crystal Growth **423**,9(2015).
[21] A., Manosa, L., Vives, E., Rodriguez-Carvajal, J., Morin, M., Guerin, G., Macqueron, J.L., ICSD using POWD-12++, Planes, Phys.: Condens. Matter, **4**, 553, (1992)
[22] Song Guang-Ling, St John D. Corrosion behavior of magnesium in ethylene glycol [J]. Corrosion Science,**46**(6), 1381 (2004).
[23] Song G L, Bowles A L, St john D H. [J].Materials Science and Engineering, **a366,** 74 (2004)
[24] Huo Hong-Wei, Li Ying, Wang Fu-Hui. [j].Corrosion Science, **46**(6), 1467 (2004)
[25] Chiu L H, Chen C C, Yang C F. [j].Surface and Coatings Technology,**191**(2/3),181 (2005)
[26]Zhang Yong-Jun, Yan Chuan-Wei, Wang Fu-Hui, Li Wen-Fang. [J].Corrosion Science, **47**(11), 2816(2005)
[27] Guo X W, Ding W J, Lu C, Zhai C Q. [J]. Surface and Coatings Technology, **183**(2/3), 359 (2004)
[28] L. Čížek , M. Greger , L.A. Dobrzański , I. Juřička ,R. Kocich , L. Pawlica , T. Tański. Journal of Achievements in Materials and Manufacturing Engineering,**18(**1-2), 203 (2006).
[29] Kainer K.U., Magnesium Alloys and Technologies, WILEY-VCH, 2003
[30]International magnesium Association, Magnesium Resources http://www.intlmag.org/magnesiumresources/alloys.cfm